Available online at www.sciencedirect.com
SCIENCE DIRECT®
Physics Letters A 324 (2004) 450–457
PHYSICS LETTERS A
www.elsevier.com/locate/pla

Phase synchronization in inhomogeneous globally coupled map lattices

Ming-Chung Ho [a], Yao-Chen Hung [b,*], I-Min Jiang [b]

[a] *Department of Physics, National Kaohsiung Normal University, Kaohsiung, Taiwan, ROC*
[b] *Department of Physics, National Sun Yat-sen University, Kaohsiung, Taiwan, ROC*

Received 6 May 2003; received in revised form 22 August 2003; accepted 9 March 2004

Communicated by A.R. Bishop

Abstract

The study of inhomogeneous-coupled chaotic systems has attracted a lot of attention recently. With simple definition of phase, we present the phase-locking behavior in ensembles of globally coupled non-identical maps. The inhomogeneous globally coupled maps consist of logistic map and tent map simultaneously. Average phase synchronization ratios, which are used to characterize the phase coherent phenomena, depend on different coupling coefficients and chaotic parameters. By using interdependence, the relationship between a single unit and the mean field is illustrated. Moreover, we take the effect of external noise and parameter mismatch into consideration and present the results by numerical simulation.

PACS: 05.45.-a; 89.75.Kd; 05.50.+q

Keywords: Phase synchronization; Globally coupled maps

1. Introduction

Coupled map lattices (CML) are often used as a convenient model to study the behavior of real spatiotemporal system [1,2]. Much work has been done in the past decades due to the rich phenomena and computational efficiency. One of the collective phenomena presented by CML is the spatiotemporal chaotic synchronization, i.e., the whole system will be coherent spatially and temporally with suitable coupling strength and chaotic parameter. This is an important subject because the similar synchronization behavior can be found in many biological, computational, physical, chemical, and even social systems.

In most of the previous studies, the identical coupled elements are considered. However, the CML consisting of identical elements are idealized and specialized cases because the subsystems in the realistic system are never identical. Recently, several papers have paid attention to inhomogeneous-coupled chaotic systems [3–5]. They present the ensemble behavior of CML, which consist of the same maps but with non-identical chaotic parameters. Based on these studies, people can understand the characteristics of realistic CML more clearly.

* Corresponding author.
E-mail address: d9123801@student.nsysu.edu.tw (Y.-C. Hung).

0375-9601/$ – see front matter
doi:10.1016/j.physleta.2004.03.017

In this Letter, we would like to explore the inhomogeneous CML further. We are interested in the lattices consisting of "different maps", not the uniform maps with different chaotic parameters. Globally coupling map lattices (GML) are considered in this Letter. With simple definition of phase [6–9], we present the phase-locking behavior in ensembles of globally coupled tent maps and logistic maps. Average phase synchronization (PS) ratios, which are used to characterize the phase coherent phenomena, depend on different coupling coefficients and chaotic parameters. By using interdependence, the relationship between a single unit and the mean field is illustrated. Moreover, we take the effect of external noise and parameter mismatch into consideration and present the results by numerical simulation.

This Letter is organized as follows. In Section 2, we describe our model and analyze the phenomena of phase synchronization. In Section 3, the conception of interdependence is introduced. In Section 4, some discussions about the robustness of PS against the external noise and parameter mismatch are contained. Finally, a brief conclusion is given.

2. Inhomogeneous GML model and PS analysis

Considering a network of N local maps under a common internal field, the system is thus a mean-field version of the CML. The explicit form of inhomogeneous GML we are going to work with is given by

$$x_{n+1}^i = (1-\varepsilon)F\big(x_n^i\big) + \frac{\varepsilon}{N}\sum_{j=1}^{N} F\big(x_n^j\big). \tag{1}$$

Here n represents a discrete time step, i and j the index of the elements ($i, j = 1, 2, \ldots, N$), and ε the coupling constant. The formula

$$\frac{1}{N}\sum_{j=1}^{N} F\big(x_n^j\big)$$

is called mean field. It is assumed that $F(x)$ gives rise to chaotic dynamic and is listed as follows:

$$\begin{cases} F\big(x_n^i\big) = f_1\big(x_n^i\big) = 1 - a_t\big|x_n^i\big|, & i \leqslant i_c, \\ F\big(x_n^i\big) = f_2\big(x_n^i\big) = 1 - a_l\big(x_n^i\big)^2, & i > i_c. \end{cases} \tag{2}$$

Tent map (f_1) or logistic maps (f_2) can be chosen as $F(x)$. For two simple reasons, we take logistic map and tent map into consideration. First, the range of x of two kinds of maps are both given by $[-1, 1]$, and the chaotic parameters a_t and a_l are within the same limits $[0, 2]$. Therefore, we do not have to normalize the value of iteration additionally to avoid system dissipation. Second, the characteristic of tent maps and logistic maps are well understood. That will help us to analyze the complex behavior more efficiently. Based on these reasons, the model is established as in Eq. (2). Critical index i_c is an operator to decide the numbers of two different maps. When $i_c = N$, the system comes back to the globally coupled tent maps. On the contrary, $i_c = 0$ presents another GML composed of logistic maps. We are familiar with these two special cases. Generally, when $0 < i_c < N$, the system is under a transitional condition between globally coupled tent maps and globally coupled logistic maps. An interesting question arisen: do the synchronization and coherent behavior of GML still exist in this transitional situation?

To answer this question, let us view the spatial and temporal evolution of global activities of the lattices. In the following, we focus our attention on a system with $N = 100$, $i_c = 50$, and start from random initial conditions. By numerical simulation, we report the case $a_t = 1.60$, $a_l = 1.65$ and $\varepsilon = 0.30$ in Fig. 1, where the five disordered signals ($i = 1, 25, 50, 75$ and 100)

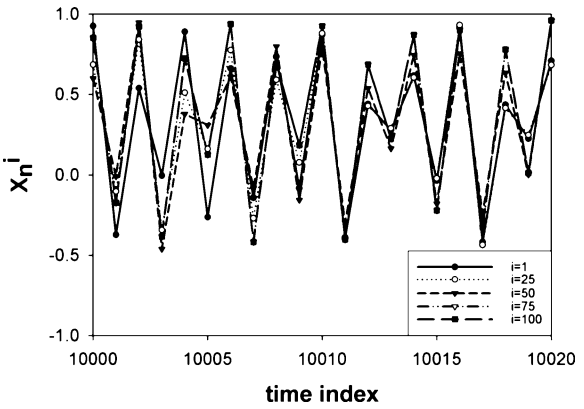

Fig. 1. Temporal evolution of the single units in the lattices for $N = 100$, $a_t = 1.60$, $a_l = 1.65$ and $\varepsilon = 0.30$. Obviously, the signals have maxima (minima) at the same time but different amplitudes. We call the state that shows local maxima (minima) at the same time as PS state.

are found. Without achieving complete synchronization, the signals present another consistency. That is, the signals show local maxima (minima) at the same time while the amplitudes of all coupled elements still display chaotic actions. Some authors defined the phenomena as phase synchronization of CML [7–9]. For a trajectory of a continuous dynamic system, the phase can be well defined by its tangent direction in the phase space. However, for discrete systems the PS phenomena are rarely studied. Stimulated by the similar idea from continuous systems, the authors give an easy and useful definition: the direction phase. For inhomogeneous GML, the direction phase of the site i at the time n is selected as [7,9]

$$S_n^i = \begin{cases} +1, & \text{if } x_{n+1}^i - x_n^i > 0, \\ -1, & \text{if } x_{n+1}^i - x_n^i \leqslant 0. \end{cases} \tag{3}$$

Here $S_n^i = 1$ means the up-phase $S_\uparrow$ and $S_n^i = -1$ means the down-phase $S_\downarrow$. When time passed by, all the elements with the same S_n^i denote the complete phase synchronization phenomenon.

To describe the PS in inhomogeneous GML more clearly, PS ratio r is used to quantitatively characterize the PS phenomenon. Let m_n^{+1} be the number of elements in phase 1 and m_n^{-1} be the number of elements in phase -1 at time index n. Now, the PS ratio is given by

$$r = \frac{1}{T}\sum_{n=1}^{T}\frac{1}{N}\left|(+1)m_n^{+1} + (-1)m_n^{-1}\right|. \tag{4}$$

Clearly, when $r = 1$, all minima and maxima of elements match each other and it corresponds to the complete phase synchronization. When r is close to zero, phase states of elements are disordered. To illuminate some special cases and get more general results, we calculate the mean value of PS ratios (called average PS ratio r_{ave}) from different initial conditions. Next, we will explore the effect of different coupling coefficients and chaotic parameters on the average PS ratio.

Fig. 2 shows the relationship between average PS ratio r_{ave} and coupling strength ε under various pairs of chaotic parameters (a_t, a_l). After sufficient transitional time, we choose $T = 20\,000$ and average the ratios with 1000 different random initial conditions at each coupling strength. The results are described as follows. (a) For $(a_t, a_l) = (1.30, 1.50)$, the

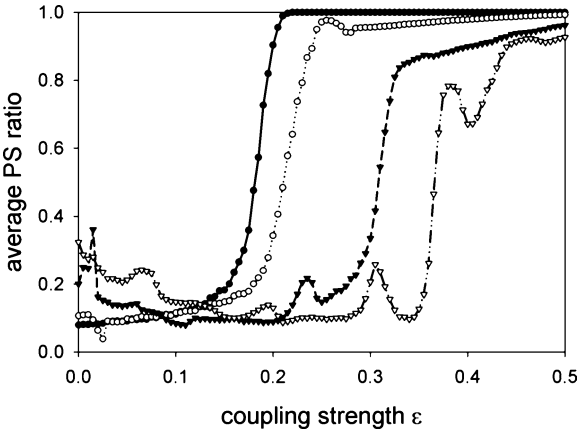

Fig. 2. The diagram shows the relationship between average PS ratio r_{ave} and coupling strength ε under various chaotic parameter pairs (a_t, a_l). Four chaotic parameters are chosen: $(a_t, a_l) = (1.30, 1.50)$ (solid circle), $(a_t, a_l) = (1.40, 1.60)$ (empty circle), $(a_t, a_l) = (1.80, 1.80)$ (solid inverted triangle) and $(a_t, a_l) = (1.99, 2.00)$ (empty inverted triangle).

average PS ratios arise quickly and equal to 1 after coupling strength $\varepsilon \geqslant 0.22$ (solid circle); that is, the complete PS is achieved after $\varepsilon \geqslant 0.22$. (b) For $(a_t, a_l) = (1.40, 1.60)$, the ratios start to increase rapidly when $\varepsilon \approx 0.20$, and diminish slightly when $\varepsilon = 0.26$ (empty circle). Then, with the increase of ε, the value of r_{ave} keeps increasing and approaches 1. (c) For $(a_t, a_l) = (1.80, 1.80)$ (solid inverted triangle) and $(1.99, 2.00)$ (empty inverted triangle), the coupling strengths where the average PS ratios begin to arise are larger than the former conditions. This is because the larger the chaotic parameter is, the harder would it compress the chaotic behavior of each element, i.e., the synchronization would be accomplished inefficiently when a_t and a_l are larger. Surprisingly, for $(a_t, a_l) = (1.99, 2.00)$ with $\varepsilon = 0.40$, the value of r_{ave} is lower than its nearby points. However, generally speaking, stronger coupling would lead to higher r_{ave}. What are the reasons? Moreover, do the systems with different sizes still present similar characteristic? Therefore, the corresponding questions are arisen: (1) why can average PS ratio not keep growing with the increase of ε? (2) How does the size N of network influence r_{ave}?

In fact, the ratios we record in Fig. 2 are the mean value of PS ratios. With regard to the first question, we choose $(a_t, a_l) = (1.99, 2.00)$ and collect the PS

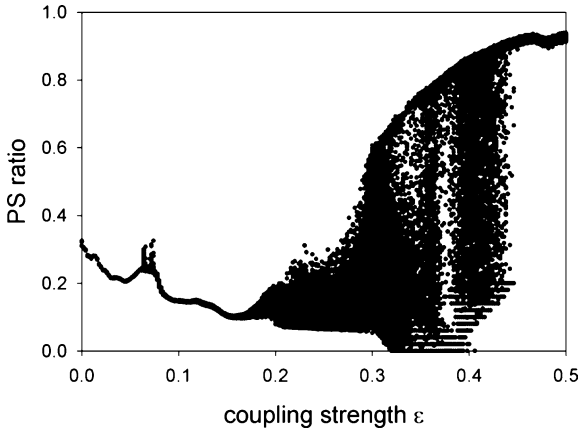

Fig. 3. For $(a_t, a_l) = (1.99, 2.00)$, we collect the PS ratios from 1000 different initial conditions instead of calculating their mean values per coupling strength. The diagram illustrates the PS ratios are extremely sensitive to the initial condition on the region $\varepsilon \in [0.19, 0.45]$.

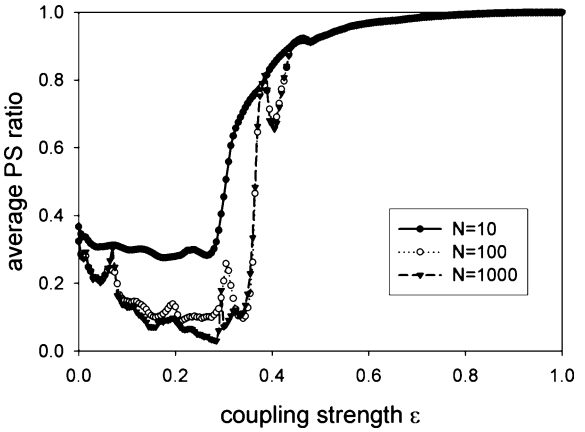

Fig. 4. Average PS ratios r_{ave} versus coupling strength with different sizes of the network N are illustrated. As shown in the diagram, the PS phenomena would not be altered by different sizes of the system with sufficient coupling.

ratios from 1000 different initial conditions instead of calculating their mean values per coupling strength. Fig. 3 illustrates the numerical results. Obviously, for $\varepsilon < 0.19$ and $\varepsilon > 0.45$, the values of r fluctuate slightly around r_{ave} in Fig. 1. For $\varepsilon \in [0.19, 0.45]$, the PS ratios are extremely sensitive to the initial condition and present an interesting structure. Due to the effect of different initial conditions, the values of PS ratio no longer fluctuate around r_{ave} slightly and the mean values no longer depend on coupling strength regularly. For instance, the values of r spread uniformly at $\varepsilon = 0.40$, whereas they present windows structure at $\varepsilon = 0.38$. That will lead to that the average PS ratio at $\varepsilon = 0.38$ is larger than it at $\varepsilon = 0.40$. The similar phenomena and structure also appear while $(a_t, a_l) = (1.80, 1.80)$ and $(a_t, a_l) = (1.40, 1.60)$.

As to the second question, we also choose $(a_t, a_l) = (1.99, 2.00)$ and compute r_{ave} under different sizes of the network. As shown in Fig. 4, we select $N = 10, 100$ and 1000, respectively. When $\varepsilon \leqslant 0.35$, the value of r_{ave} for $N = 10$ is larger than $N = 100$, and it for $N = 100$ is larger than $N = 1000$. It is reasonable because the interaction behavior of an ensemble of larger coupled units is more complex than that of a fewer units. However, after $\varepsilon > 0.35$, the ensemble phase behavior for $N = 1000$ begins to agree with $N = 100$ under the compress force from mean field; after $\varepsilon > 0.45$, the size of network almost has nothing to do with r_{ave}. That is, the PS phenomena would not be altered by different sizes of the system with sufficient coupling.

As we can find above, the chaotic parameter pairs (a_t, a_l) play important roles in phase synchronization of the ensemble system. In the following, we will investigate the relationships among average PS ratios, parameter a_t and a_l. Having coupling strength equal to 0.30, we calculate r_{ave} under the condition used in Fig. 2. Choosing $a_t \in [1.1, 2.0]$ and $a_l \in [1.4, 2.0]$, all elements are sure to present chaotic behavior. To describe the details more clearly, $\ln(1/r_{\text{ave}})$ is used to replace average PS ratios r_{ave} to demonstrate the relationship. Results are illustrated in Fig. 5. $\ln(1/r_{\text{ave}}) = 0$ corresponds to the complete phase synchronization situation. On the contrary, when the value of $\ln(1/r_{\text{ave}})$ becomes larger, the phase states of the whole system get more turbulent. In Fig. 5, phase synchronization occurs in a range of parameter values, and coherent behaviors gradually lost as the values of (a_t, a_l) increase. After $a_t > 1.60$ and $a_l > 1.60$, no complete phase synchronization is found. It means the driving force of mean field fails to compress the complexity within this parameter region. The relationships among average PS ratio, parameters a_t and a_l are irregular. For instance, as $a_l > 1.60$, the values of $\ln(1/r_{\text{ave}})$ for $a_t \approx 1.20$ correspond to a "valley" terrain while for $a_t \approx 1.95$ correspond to a "mountaintop" terrain. Why? We expect the problem

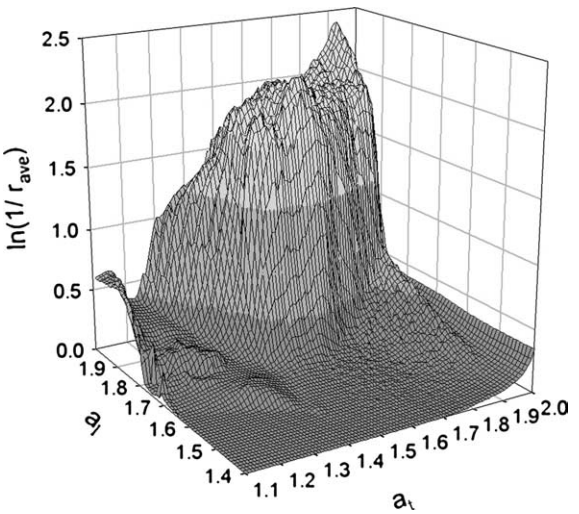

Fig. 5. With fixed coupling strength $\varepsilon = 0.30$, the relationships among $\ln(1/r_{\text{ave}})$, parameter a_t and a_l are presented. $\ln(1/r_{\text{ave}}) = 0$ corresponds to the complete phase synchronization situation. On the contrary, when the value of $\ln(1/r_{\text{ave}})$ becomes larger, the phase states of the whole system get more turbulent.

can be solved by analyzing the structure of two maps further. More thorough researches will be done in the future.

3. Interdependence

In this section, the conception of interdependence is introduced to illustrate the relationship between a single unit and the mean field. Let us assume we have two simultaneously measured time series from which we can reconstruct m-dimensional delay vectors [10] $\mathbf{x}_n = (x_n, \ldots, x_{n+m-1})$ and $\mathbf{y}_n = (y_n, \ldots, y_{n+m-1})$, where n represents a discrete time step. Let $r_{n,j}$ and $s_{n,j}$, $j = 1, \ldots, k$, denote the time indices of the k nearest neighbors of $\mathbf{x}_n$ and $\mathbf{y}_n$. To $\mathbf{x}_n$, the squared mean distance from these neighbors is then given as [11–13]

$$R_n^{(k)}(X) = \frac{1}{k}\sum_{j=1}^{k}\left(\mathbf{x}_n - \mathbf{x}_{r_{n,j}}\right)^2. \tag{5}$$

Analogously, $R_i^{(k)}(Y)$ can be defined by exchanging X and Y. Further, the "conditional" distance

$$R_n^{(k)}(X/Y) = \frac{1}{k}\sum_{j=1}^{k}\left(\mathbf{x}_n - \mathbf{x}_{s_{n,j}}\right)^2 \tag{6}$$

can be defined. The only difference between Eq. (5) and Eq. (6) is the indices used in the second term. Furthermore, $R_n^{(k)}(X/Y) \approx R_n^{(k)}(X)$ if the systems are strongly correlated. When two systems are independent, we can expect $R_n^{(k)}(X/Y) \gg R_n^{(k)}(X)$. Now, a measure for dependence can be defined as

$$S^{(k)}(X/Y) = \frac{1}{T}\sum_{n=1}^{T}\frac{R_n^{(k)}(X)}{R_n^{(k)}(X/Y)}. \tag{7}$$

The value of S ranges from nearly zero (for independent systems) to one (for strongly dependent or identical systems). Another interdependence measure with similar properties is

$$H^{(k)}(X/Y) = \frac{1}{T}\sum_{n=1}^{T}\ln\frac{R_n(X)}{R_n^{(k)}(X/Y)}, \tag{8}$$

which differs from S in comparing the conditional distance with the mean distance of all points for $\mathbf{x}_n$. While both qualities have proven to be useful in real data applications, H is more beneficial to judge the direction of information transformation [12]. In this Letter, we will use the definition of H to research the correlation between a single unit and the mean field.

Taking the time series of x^1(the single unit with $i = 1$) as $\mathbf{x}_n$ and the mean field as $\mathbf{y}_n$, we calculate interdependence $H^{(k)}(X/Y)$ and $H^{(k)}(Y/X)$ in different parameter pairs numerically. In order to eliminate transitional signals, sufficient iterations were discarded. Interdependencies were then estimated from $T = 5000$ iterations using three-dimensional delay vectors and $k = 20$ nearest neighbors. Similarly, all computations were repeated several times with different initial conditions. Fig. 6 shows $H^{(k)}(X/Y)$ and $H^{(k)}(Y/X)$ for $(a_t, a_l) = (1.99, 2.00)$ (Fig. 6(a)) and $(a_t, a_l) = (1.30, 1.50)$ (Fig. 6(b)) as functions of the coupling strength ε. Solid line with filled circles is for $H^{(k)}(X/Y)$, whereas dash line with empty circles is for $H^{(k)}(Y/X)$. Comparing Fig. 6 with Fig. 2 and Fig. 4, it is easy to observe that interdependence agree with average PS ratios. Our results can be understood by following arguments.

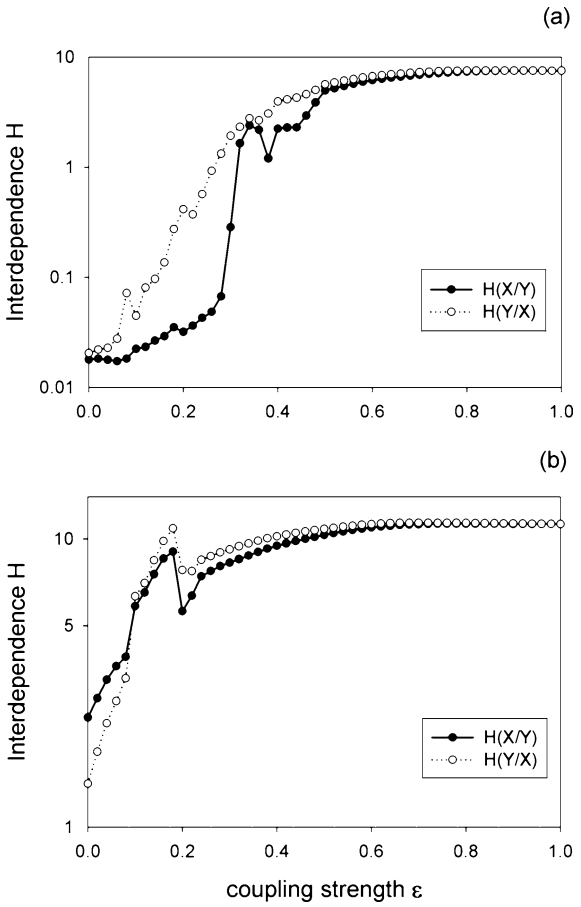

Fig. 6. Nonlinear interdependence $H^{(k)}(X/Y)$ and $H^{(k)}(Y/X)$ between the single unit ($i = 1$) and the mean field for (a) $(a_t, a_l) = (1.99, 2.00)$ and (b) $(a_t, a_l) = (1.30, 1.50)$. We take the time series of x^1 (the single unit with $i = 1$) as $\mathbf{x}_n$ and the mean field as $\mathbf{y}_n$.

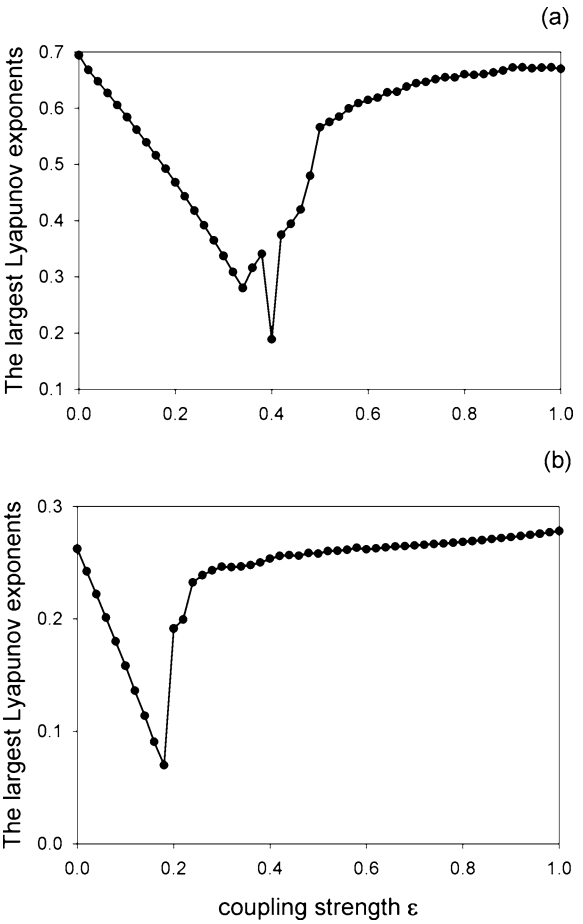

Fig. 7. The largest Lyapunov exponents as a function of coupling strength for (a) $(a_t, a_l) = (1.99, 2.00)$, and for (b) $(a_t, a_l) = (1.30, 1.50)$. The flat part corresponds to the phase synchronization state.

(1) In Fig. 6(a), we select $(a_t, a_l) = (1.99, 2.00)$ as the chaotic parameter pair. For $\varepsilon \geqslant 0.30$, we can see a sharp increase of $H^{(k)}(X/Y)$, whereas r_{ave} in Fig. 4 starts to rise at the same coupling strength. For $\varepsilon \geqslant 0.40$, $H^{(k)}(X/Y)$ increase slowly and keep rising lightly after $\varepsilon \geqslant 0.50$. The similar behaviors also can be viewed in the relationship between r_{ave} and ε in Fig. 4.

(2) Fig. 6(b) presents the results under $(a_t, a_l) = (1.30, 1.50)$. After $\varepsilon \geqslant 0.24$, the values of $H^{(k)}(X/Y)$ and $H^{(k)}(Y/X)$ reach more steady states, which correspond to the phase coherent states, and keep growing gradually with the increase of coupling strength. At intervals $\varepsilon \in [0.10, 0.18]$, $H^{(k)}(X/Y)$ and $H^{(k)}(Y/X)$ enlarge unusually and become higher than nearby points, but r_{ave} do not show the same behavior. This is because single units and mean field present 4-periods-like iterations under the condition $(a_t, a_l) = (1.30, 1.50)$ and $\varepsilon \in [0.10, 0.18]$. Due to this, the correlations among them are stronger than in chaotic cases.

(3) The main advantage H has over other similar measures for dependence is its asymmetry, i.e., the asymmetry can help us to determine the "direction" of the coupling. If $H^{(k)}(X/Y) > H^{(k)}(Y/X)$, we just say that $\mathbf{y}_n$ is more active than $\mathbf{x}_n$. In fact, the

system with higher dimension should be more active, and the response system usually does have higher dimension. In Fig. 6, the inequality $H^{(k)}(Y/X) > H^{(k)}(X/Y)$ satisfies except extreme strong or weak coupling. For strong coupling, the two systems are synchronized and it is hard to judge the direction. As for weak coupling, the values of H depend on the original dimension of the system. Therefore, from the inequality $H^{(k)}(Y/X) > H^{(k)}(X/Y)$, we can say $\mathbf{x}_n$ is more active than $\mathbf{y}_n$. In other words, the direction of coupling is from mean field to a single unit. As the result of the common driving force from the mean field, the PS phenomena are generated in inhomogeneous globally coupled maps. Actually, by means of interdependence, we can verify the concept more exactly and identify the relationship between a single unit and the mean field.

In addition, interdependence also connects well with the largest Lyapunov exponents. Fig. 7(a) illustrates the relationship between the largest Lyapunov exponents and the coupling strength for $(a_t, a_l) = (1.99, 2.00)$ while Fig. 7(b) does for $(a_t, a_l) = (1.30, 1.50)$. Unlike continuous oscillators, the plate part in the figure corresponds to the coherent state [14]. In other words, for $(a_t, a_l) = (1.99, 2.00)$ the phase synchronization states achieved after $\varepsilon \geqslant 0.5$. The results agree with what we get above. Similar connections can be observed for $(a_t, a_l) = (1.30, 1.50)$.

4. Robustness

In real physical systems, it is impossible to eliminate the effect of external noise and parameter mismatch. Here we consider the two cases and observe the variation of whole system under these fluctuations. For external noise, the inhomogeneous model can be rewritten as

$$x_{n+1}^i = (1-\varepsilon)F\left(x_n^i\right) + \frac{\varepsilon}{N}\sum_{j=1}^{N} F\left(x_n^j\right) + \xi_n^i, \tag{9}$$

for the ith element at time step n. We adopt Gaussian random process for ξ_n^i with $\langle \xi_n^i \rangle = 0$ and $\langle \xi_n^i \xi_m^j \rangle = \sigma^2 \delta_{nm} \delta_{ij}$. The variance of Gaussian distribution is denoted by σ^2 [15]. Taking account of parameter mismatch, Eq. (2) turns out to be

$$\begin{cases} F\left(x_n^i\right) = f_1\left(x_n^i\right) = 1 - a_t\left(1+\alpha\eta^i\right)\left|x_n^i\right|, & i \leqslant i_c, \\ F\left(x_n^i\right) = f_2\left(x_n^i\right) = 1 - a_l\left(1+\alpha\eta^i\right)\left(x_n^i\right)^2, & i > i_c. \end{cases} \tag{10}$$

α denotes the detuning coefficient of parameter and η^i a random number between -1 and 1, thus η^i is different for each unit.

Our numerical results show that external noise has nothing to do with phase synchronization, i.e., the relationship between average PS ratios and coupling strength are almost the same under the effect of external noise. The similar situations also happen to chaotic parameter mismatch. Fig. 8 shows the outcomes of the parameter mismatch under $(a_t, a_l) = (1.30, 1.50)$

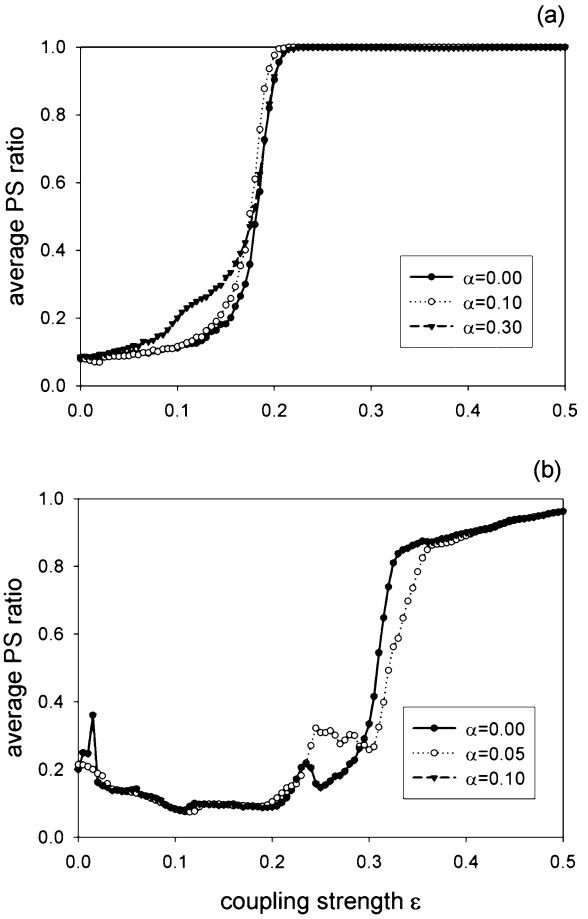

Fig. 8. The diagram shows the outcomes of the parameter mismatch under (a) $(a_t, a_l) = (1.30, 1.50)$ and (b) $(a_t, a_l) = (1.80, 1.80)$. It illustrates that PS has sufficient robustness against the parameter mismatch.

and $(a_t, a_l) = (1.80, 1.80)$. For $(a_t, a_l) = (1.30, 1.50)$, we choose $\alpha = 0.00$ (without any mismatch), 0.10 and 0.30, respectively. One can see that r_{ave} under $\alpha = 0.10$ and 0.30 are approximately the same while they are under $\alpha = 0.00$ except for some fluctuations. For the more chaotic situation, $(a_t, a_l) = (1.80, 1.80)$, the phase synchronization cannot be destroyed, either. It illustrates that PS has sufficient robustness against such mismatch.

On the other hand, because of the fluctuation of the parameters, the whole system conforms to what we call the "inhomogeneous" globally coupled maps lattices. As shown above, the phase coherent behaviors do persist robustly.

5. Conclusions

To sum up, we have shown the PS behavior in inhomogeneous globally coupled map lattices (consisted with logistic maps and tent maps simultaneously). Using the simple definition of phase direction and phase ratios, we characterize the PS under different chaotic parameters, coupling strengths and the sizes of the network. Besides, the interdependence of a single unit and the mean field is under our discussion. Finally, we present the effect of external noise and parameter mismatch and the strong robustness of phase coherent behaviors.

Acknowledgements

The authors would like to thank the National Science Council, Taiwan, ROC, for financially supporting this research under Contract No. NSC 91-2112-M-017-002.

References

[1] K. Kaneko, Chaos 2 (1992).
[2] K. Kaneko, Theory and Applications of Coupled Map Lattices, Wiley, Chichester, 1993.
[3] G.V. Osipov, J. Kurths, Phys. Rev. E 65 (2001) 016216.
[4] A. Sharma, N. Gupte, Phys. Rev. E 66 (2002) 036210.
[5] J. Dacidsen, R. Kapral, Phys. Rev. E 66 (2002) 055202(R).
[6] M.G. Rosenblum, A.S. Pikovsky, J. Kurths, Phys. Rev. Lett. 76 (1996) 1804.
[7] W. Wang, Z. Liu, B. Hu, Phys. Rev. Lett. 84 (2000) 2610.
[8] B. Hu, Z. Liu, Phys. Rev. E 62 (2000) 2114.
[9] G. Zhuang, J. Wang, Y. Shi, W. Wang, Phys. Rev. E 66 (2002) 046201.
[10] H.D.I. Abarbanel, Analysis of Chaotic Time Series, Springer, Berlin, 1996.
[11] R. Quian Quiroga, J. Arnhold, P. Grassberger, Phys. Rev. E 61 (2000) 5142.
[12] A. Schmitz, Phys. Rev. E 62 (2000) 7508.
[13] M.C. Ho, F.C. Shin, Phys. Rev. E 67 (2003) 056214.
[14] S. Morita, Phys. Lett. A 226 (1997) 172.
[15] T. Shibata, T. Chawanya, K. Kaneko, Phys. Rev. Lett. 82 (1999) 4424.